ELSEVIER

Biochimica et Biophysica Acta 1421 (1999) 295–305

BIOCHIMICA ET BIOPHYSICA ACTA
BBA

www.elsevier.com/locate/bba

The transmembrane protein bacterioopsin affects the polarity of the hydrophobic core of the host lipid bilayer

Fabrice Dumas, Maria-Chantal Lebrun, Pascale Peyron, André Lopez, Jean-François Tocanne *

Institut de Pharmacologie et Biologie Structurale du CNRS, 118 Route de Narbonne, F-31062 Toulouse Cedex France

Received 19 January 1999; received in revised form 23 July 1999; accepted 5 August 1999

Abstract

Influence of the transmembrane protein bacterioopsin (the retinal-free form of bacteriorhodopsin) on the polarity of egg-phosphatidylcholine bilayers was studied by means of a steady-state and time-resolved fluorescence approach exploiting the solvatochromic properties of the 2-anthroyl fluorophore. Introduced in phosphatidylcholine molecules in the form of 8-(2-anthroyl)octanoic acid, this fluorophore probed the hydrocarbon core of the lipid bilayer. As previously shown (E. Pérochon et al., Biochemistry 31 (1992) 7672–7682), water molecules were detected in this region of the terminal part of the lipid acyl chains. Their number was considerably reduced upon addition of bacterioopsin to the lipids. This was assessed by a blue shift in the fluorescence emission spectra of the probe and a marked decrease in the fractional population of fluorophores interacting with water, to the benefit of those experiencing a hydrophobic environment. In agreement with current theories, this decrease in the hydration of the bilayer may be linked to an increase in the acyl chain order and a decrease in the lateral diffusion coefficient of lipids near the protein. The data obtained at high protein concentration accounts for a protein/lipid interface which is much less hydrated than the hydrophobic core of a protein-free lipid bilayer.

Keywords: Bacterioopsin; Bacteriorhodopsin; Protein–lipid interaction; Water permeability; Fluorescence; Lateral diffusion; 2-Anthroyl chromophore

1. Introduction

It has long been recognized that lipid bilayers display permeability to water [1–3]. Diffusion across the hydrophobic barrier occurs rapidly and on the average water molecules are present in the hydrophobic core of the bilayer, intercalated between the lipid acyl chains [3–5]. However, because of their relatively low number and high mobility, these diffusing water molecules are difficult to observe and their detection requires specific and highly sensitive methods. Fluorescence is one of the best suited approaches [5,6] and in this respect, we have introduced the 2-anthroyl fluorophore in the form of 8-(2-anthroyl)octanoic acid [7] as a polarity probe because of the remarkable solvatochromic properties it displays. Thus, when going from hexane to water, the maximum fluores-

Abbreviations: DMPC, dimyristoylphosphatidylcholine; DOPC, dioleoylphosphatidylcholine; egg-PC, egg yolk phosphatidylcholine; anthroyl-PC, 1-acyl-2-[8-(2-anthroyl)octanoyl]-*sn*-glycero-3-phosphocholine; CHAPS, 3-[(3-cholamidopropyl)dimethylammonio]-1-propane-sulfonate; POPOP, *p*-bis(5-phenyl-2-oxazolyl)benzene

* Corresponding author. Fax: +33-05-61-33-58-86;
E-mail: tocanne@ipbs.fr

0005-2736/99/$ – see front matter
PII: S0005-2736(99)00133-9

cence emission wavelength shifts from 404 nm to 526 nm, the relative quantum yield, ϕ, increases from 1 to 27 and the fluorescence lifetime, τ, from 1 ns to 20 ns [7]. Phosphatidylcholine labeled with 8-(2-anthroyl)-octanoic acid (anthroyl-PC) has been synthesized and its phase and fluorescence properties have been carefully investigated [7,8]. In the configuration used (the aromatic rings and the polymethylenic chain lie along the same axis), anthracene is poorly disturbing for the surrounding lipids and anthroyl-PC behaves like a normal phospholipid. The probe exhibits good miscibility with lipids [8] and no preference for lipids in the disordered or ordered states [30]. In bilayers, and from fluorescence quenching experiments, the chromophore is located in depth where expected, i.e., along the C9–C16 segment of the acyl chains [5]. On these grounds, steady-state and time-resolved fluorescence experiments carried out with anthroyl-PC in egg-PC vesicles clearly showed the presence of water in the hydrophobic core of the lipid bilayers: the probe experienced at least three different and quite distinct environments, two of hydrophobic nature and the third corresponding to interactions with water molecules diffusing across the lipid bilayer [5].

The mechanisms underlying water diffusion across lipid bilayers are far from well understood. However, evidence is accumulating which indicates that water permeability is strongly related to the packing density of lipids, in relation to the nature and movements of their polar headgroups and acyl chains [4,9–15]. In this respect, cholesterol which is known to increase the acyl chain order of lipids [16] has also been shown to decrease their permeability to water [9,10,13,17,18]. Accordingly, addition of cholesterol to egg-PC vesicles increased the fractional population of anthroyl-PC molecules experiencing a hydrophobic environment at the expense of those interacting with water [5].

Although proteins are massively present in biological membranes, their influence on the hydration and permeability to water of the lipid bilayer remains poorly documented [9,19]. However, proteins are known to affect the translational [20,21] and conformational [22,23] motions of lipids and thereby changes in the hydration of the bilayer should occur. In the present study, and by means of the above fluorescence approach, we show that bacterioopsin, the retinal-free form of the transmembrane protein bacteriorhodopsin, decreases the hydration of egg-PC bilayers in its proximity, as cholesterol does, and that the protein/lipid interface is much less hydrated than the hydrophobic core of the bulk lipids.

2. Materials and methods

2.1. Chemicals

Syntheses of methyl 8-(2-anthroyl)octanoate and corresponding anthroyl-PC have already been described [8]. Egg-PC was obtained from Sigma Chemical Co. (St. Louis, MO, USA). Its purity was checked by thin-layer chromatography on silica gel plates. It was used without further purification. Solvents were of analytical grade.

2.2. Preparation of purple membrane and apomembrane

Purple membrane fragments were isolated from *Halobacterium halobium* according to well-established procedures [24]. Partial delipidation was achieved by incubation in the presence of CHAPS 1% (w/v). After 48 h contact, the detergent was removed by adsorption on hydrophobic resins (SM2 Biobeads, 2 h contact) [25] and the membrane fragments were washed twice and resuspended in acetate buffer (100 mM Na-acetate, 150 mM NaCl, pH 5.0). Determination of the protein [26] and phosphorus [27] content showed that one molecule of bacteriorhodopsin remained associated with approximately 3 molecules of phospholipids as compared to about 10 molecules in the native purple membrane.

Bacterioopsin, the retinal-free form of bacteriorhodopsin, was prepared by illumination of purple membrane fragments at a concentration of 2×10^{-5} M with a halogen lamp (KL 1500 electronic, Schott) in the presence of 2 M hydroxylamine at pH 7 [25]. After the purple color had completely disappeared, membrane fragments were collected by centrifugation, washed twice with the acetate buffer and then used for reconstitution experiments.

2.3. Reconstitution of bacterioopsin in lipid vesicles

Bacterioopsin was reconstituted in egg-PC vesicles

and in the presence of 1 mol% anthroyl-PC with respect to the lipids, exactly as described for bacteriorhodopsin [25]. To prevent the formation of lipid peroxides, care was taken to use peroxide-free diethylether and to perform experiments in the presence of nitrogen [25]. The bacterioopsin to lipid molar ratio was varied from 1:250 to 1:18. Homogeneity and composition of the proteoliposomes were checked after ultracentrifugation of the various preparations on a linear sucrose gradient (5–40%) [25]. In most cases, a single and sharp band was observed. Its protein content was analyzed according to [26] and phospholipids were assayed by measuring the fluorescence of the anthroyl-PC probe. More than 90% of the reconstituted vesicles were found to be composed mainly ($\sim$95%) of proteoliposomes of uniform density (the sharp band corresponded in fact to a small volume of less than 0.1 ml for a total volume of 11 ml) and with the expected bacterioopsin/egg-PC composition. In these preparations, non-reconstituted protein was absent and the non-proteoliposome material ($\sim$5%) corresponded to protein-free lipid vesicles. Absence of lipid peroxidation was assessed spectroscopically by the absence of the characteristic absorption band at 220–230 nm [28]. The samples (less than 10%) which did not meet these criteria of homogeneity and composition were discarded.

2.4. Fluorescence spectrophotometry

Fluorescence emission spectra were recorded with a SLM-Aminco spectrofluorimeter, model 500. Slit widths of 1 nm were used for all measurements. Absorbance of the proteoliposome suspensions was around 0.05 and never greater than 0.1 in the 350–700 nm wavelength range. Absorption spectra were recorded with a Perkin–Elmer Lambda 16 UV/Visible spectrometer. Experiments were carried out at 20°C.

2.5. Fluorescence Lifetime measurements

Fluorescence decays were monitored by a single photon counting technique and using an apparatus which has been described elsewhere [5,29]. The excitation beam was produced by a picosecond mode-locked titanium/sapphire laser. A pulse repetition rate of 800 kHz was used. The excitation wavelength was 380 nm and fluorescence was recorded at 450 nm with a monochromator (slit width: 5 nm) coupled to a Philips 2020 photomultiplier tube. The apparatus response function was evaluated by reference to the fluorescence decay of POPOP in ethanol (τ=1.35 ns) [5]. Decays were recorded over a time range of 100 ns and dispatched over the 1024 channels of the multichannel analyzer. After deconvolution of the apparatus response function, decays were analyzed as the sum of a finite number of exponentials, using a least-square algorithm including a ponderation function taking into account the fact that the noise of photon counting obeys a Poisson law of distribution [5,29]. Coupled with statistical analysis of the data, this procedure enabled us to calculate the characteristic time τ_i and the steady-state intensity I_i of each exponential according to the following equation:

$$I(t) = \sum_{i=1}^{i=n} I_i/\tau_i \exp(-t/\tau_i) \text{ with } I_i/\tau_i = \alpha_i \quad (1)$$

In the following, I_i and τ_i are given with an error risk of 5%.

When necessary, mean fluorescence lifetimes $\langle\tau\rangle$ were calculated as [30]:

$$\langle\tau\rangle = \sum I_i\tau_i / \sum I_i \quad (2)$$

2.6. Fluorescence polarization experiments

Experiments were carried out with a T-format automatic apparatus of our fabrication which has been described elsewhere [31]. The excitation wavelength was 360 nm and fluorescence was measured over the 400–500 nm wavelength range. Fluorescence anisotropy r is given as

$$r = (I_{\parallel} - I_{\perp})/(I_{\parallel} + 2I_{\perp}) \quad (3)$$

3. Results

Because of a significant overlap between the fluorescence emission spectra of the 2-anthroyl chromophore and the absorption spectrum of retinal, a mechanism of fluorescence energy transfer is ex-

pected when using bacteriorhodopsin, and in a way which depends on the protein/lipid ratio. Such consequences on the probe response would make any interpretation of the fluorescence data in terms of polarity difficult. To circumvent this drawback, experiments were carried out with bacterioopsin, the retinal-free form of bacteriorhodopsin, a molecule which does not absorb light over the 380–650 nm wavelength range where the fluorescence emission of the 2-anthroyl fluorophore may occur [7].

3.1. Fluorescence spectra

In egg-PC alone (Fig. 1), and as previously observed [5], anthroyl-PC exhibited a broad steady-state fluorescence emission spectrum with a maximum emission wavelength λ_{em}^{max} around 464 nm, above that of 404 nm expected for a hydrophobic environment [7] and indicating a relatively polar environment for the probe in the lipid bilayer [5]. Actually, and as explained in details in the Discussion, this spectrum was shown to be the sum of three well-resolved decay associated spectra (DAS) corresponding to three distinct environments for the probe, two of hydrophobic nature and the third corresponding

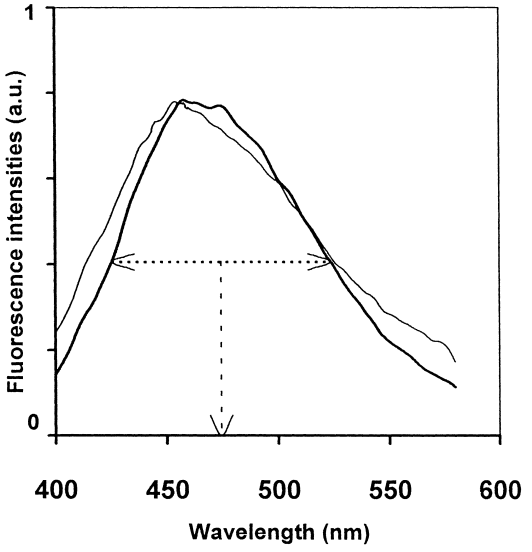

Fig. 1. Normalized fluorescence emission spectra of anthroyl-PC (1 mol%) in vesicles of egg-PC alone (thick line) and after addition of bacterioopsin (thin line) at the protein/lipid ratio of 1:50. $\lambda_{1/2}$ corresponds to the middle of the width of the spectrum at half maximum intensity. λ_{ex} was 340 nm and the temperature was 20°C.

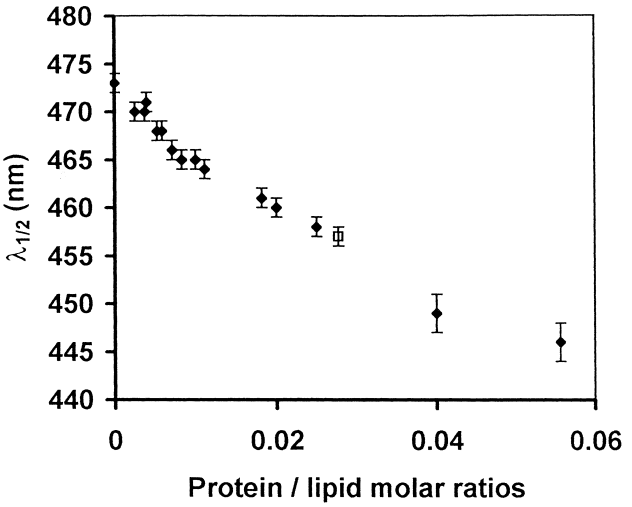

Fig. 2. Influence of bacterioopsin on $\lambda_{1/2}$ (see legend to Fig. 1) of anthroyl-PC (1 mol%) in egg-PC vesicles (♦). □, Data obtained in the presence of non-delipidated bacterioopsin.

to interactions with water molecules diffusing across the lipid bilayer [5].

Addition of bacterioopsin to the lipids resulted in an overall blue shift of the spectra which was evidenced by plotting the wavelength $\lambda_{1/2}$ corresponding to the middle of the width of each spectrum at half maximum intensity. As can be seen in Fig. 2 and Table 1, $\lambda_{1/2}$ progressively decreased upon addition of bacterioopsin to the lipids, from 473 nm for egg-PC alone down to 446 nm for the protein/lipid molar ratio of 1:18 (the highest we tested), indicating a decrease in the apparent polarity of the probe environment.

3.2. Fluorescence decays

It is worth stressing that in all cases, and as previously observed [5], best fitting of the fluorescence decays was achieved using three exponentials (χ^2 values < 1.6, Table 1). Using four exponentials resulted in the splitting of one of the three previous lifetime populations (τ_i, α_i), into two subpopulations (i_1 and i_2) of the same lifetime ($\tau_{i1} = \tau_{i2} = \tau_i$) and corresponding fractional intensity ($\alpha_{i1} + \alpha_{i2} = \alpha_i$).

In egg-PC alone, anthroyl-PC showed fluorescence lifetimes of 1.3 ns, 5.8 ns and 20.1 ns (Fig. 3, Table 1). They were similar to those of 1.5 ns, 5.5 ns and 20 ns previously reported for the probe in the same lipid [5] and were shown to account for three distinct

Table 1
Steady-state and time-resolved fluorescence characteristics of anthroyl-PC (1 mol%) in egg-PC vesicles in the absence and presence of bacterioopsin

Protein/lipid ratios	r	$\lambda_{1/2}$ (nm)	τ_1 (ns)	I_1	τ_2 (ns)	I_2	τ_3 (ns)	I_3	χ^2	$\langle\tau\rangle$ (ns)
0	0.100	473 ± 1	1.33 ± 0.07	0.08 ± 0.01	5.79 ± 0.28	0.17 ± 0.01	20.1 ± 0.8	0.75 ± 0.02	1.094	16.07
1:395		470 ± 1	1.33 ± 0.07	0.09 ± 0.01	5.79 ± 0.28	0.18 ± 0.01	20.1 ± 0.8	0.73 ± 0.02	1.124	15.83
1:265		470 ± 1	1.32 ± 0.07	0.09 ± 0.01	4.99 ± 0.22	0.21 ± 0.01	19.6 ± 0.7	0.70 ± 0.02	1.316	14.90
1:250		471 ± 1	1.21 ± 0.06	0.11 ± 0.01	5.01 ± 0.22	0.24 ± 0.01	19.2 ± 0.7	0.64 ± 0.02	1.157	13.64
1:190		468 ± 1	0.97 ± 0.05	0.07 ± 0.01	5.15 ± 0.23	0.21 ± 0.01	19.3 ± 0.7	0.72 ± 0.02	1.099	15.05
1:170		468 ± 1	1.55 ± 0.08	0.10 ± 0.01	5.91 ± 0.28	0.19 ± 0.01	19.4 ± 0.7	0.71 ± 0.02	1.415	15.05
1:140		466 ± 1	1.53 ± 0.08	0.15 ± 0.01	5.89 ± 0.28	0.26 ± 0.01	18.9 ± 0.7	0.59 ± 0.02	1.407	12.92
1:120	0.110	465 ± 1	2.77 ± 0.11	0.19 ± 0.01	7.44 ± 0.35	0.25 ± 0.01	18.8 ± 0.7	0.56 ± 0.02	1.530	12.94
1:100	0.116	465 ± 1	1.70 ± 0.08	0.23 ± 0.01	6.78 ± 0.28	0.31 ± 0.01	19.6 ± 0.7	0.46 ± 0.02	1.320	11.79
1:90		464 ± 1	1.76 ± 0.08	0.19 ± 0.01	7.5 ± 0.35	0.30 ± 0.01	17.6 ± 0.6	0.51 ± 0.02	1.372	10.23
1:55		462 ± 1	2.38 ± 0.11	0.22 ± 0.01	7.65 ± 0.34	0.29 ± 0.01	18.5 ± 0.7	0.44 ± 0.02	1.514	12.18
1:50	0.207	462 ± 1	2.74 ± 0.11	0.29 ± 0.01	6.58 ± 0.30	0.25 ± 0.01	16.6 ± 0.6	0.46 ± 0.02	1.625	9.84
1:40	0.198	461 ± 2	2.2 ± 0.11	0.29 ± 0.01	5.39 ± 0.28	0.31 ± 0.01	15.6 ± 0.6	0.40 ± 0.02	1.499	8.26
1:25	0.206	449 ± 2	2.08 ± 0.14	0.31 ± 0.01	5.85 ± 0.31	0.31 ± 0.02	15.0 ± 0.7	0.38 ± 0.02	1.639	8.22
1:18		446 ± 1	1.79 ± 0.13	0.28 ± 0.02	4.95 ± 0.33	0.30 ± 0.02	14.3 ± 0.8	0.41 ± 0.02	1.587	7.88
1:36[a]		459 ± 1	1.89 ± 0.11	0.31 ± 0.01	5.24 ± 0.25	0.30 ± 0.01	15.2 ± 0.6	0.39 ± 0.02	1.603	8.07

r is the fluorescence anisotropy. $\lambda_{1/2}$ corresponds to the middle of the width of the emission spectra at half maximum intensity. τ_i and I_i are the fluorescence lifetimes and fractional fluorescence intensities, respectively. $\langle\tau\rangle$ is the mean fluorescence lifetime.
[a]Data obtained in the presence of non-delipidated bacterioopsin.

probe environments [5]. Upon addition of bacterioopsin to the lipids, the short and intermediate lifetimes remained unchanged around a central value of ~2 ns and ~6 ns, respectively, while the long one progressively decreased, down to a value of 14.3 ns for the 1:18 protein/lipid ratio (Fig. 3, Table 1).

It should be remembered that bacteriorhodopsin was delipidated in the presence of CHAPS. On account of the procedure used for the preparation of bacterioopsin, residual CHAPS concentration may be estimated to be less than 0.01 mol% with respect to the protein which means at the most, less than 0.2 mol% with respect to the lipids. However, to rule out any possible influence of CHAPS on the structure of the lipid bilayer (the few residual molecules which might be brought by the protein), the probe fluorescence response in egg-PC vesicles was tested in the presence of increasing CHAPS concentration in the aqueous phase. Up to the high CHAPS concentration of 5 mol% with respect to the lipids, the probe showed unaltered λ_{em}^{max}, τ_i, and I_i values (data not shown), thus allowing us to discard any contribution of residual CHAPS molecules (if any) on the fluorescence signal in the presence of bacterioopsin. Because the purple membrane was not completely delipidated, the question also arose of a possible perturbation of the lipid bilayer by the remaining endogenous lipids, especially at high protein/lipid ratios. Ac-

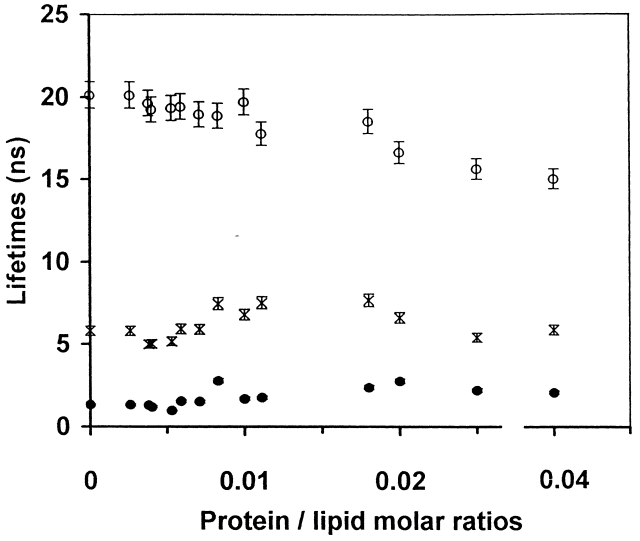

Fig. 3. Fluorescence lifetimes measured for anthroyl-PC (short (●), intermediate (×) and long (○) lifetimes) in egg-PC vesicles in the presence of increasing amounts of bacterioopsin. λ_{ex} was 380 nm and λ_{em} was 450 nm. Temperature was 20°C. For the short and intermediate lifetimes, the error bars are within the size of the symbols.

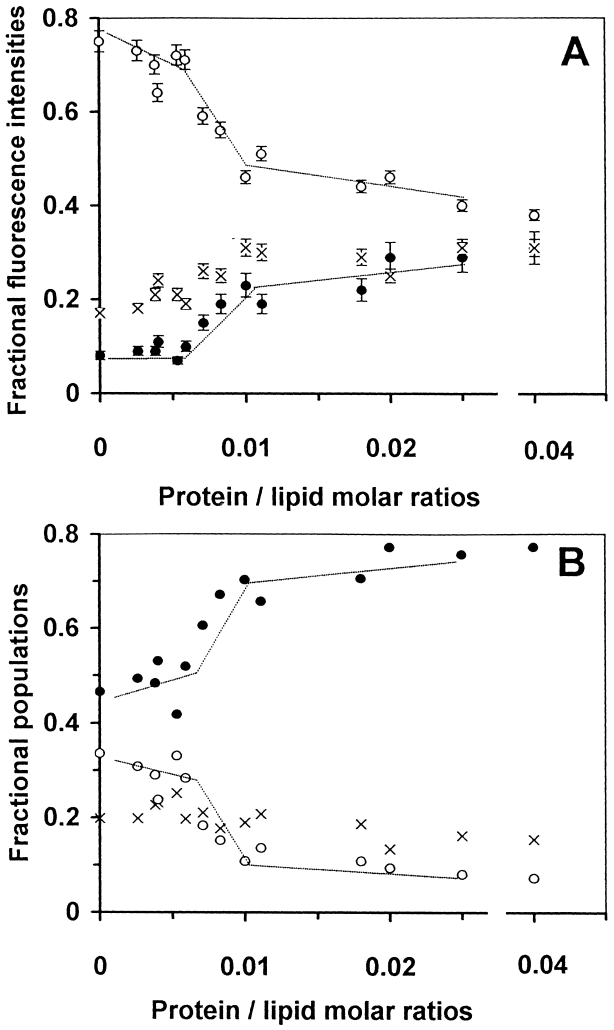

Fig. 4. Influence of bacterioopsin on the fractional fluorescence intensities (A) and probe population (B) associated with the short (●), intermediate (×) and long (○) lifetimes shown in Fig. 3. Data in B were obtained by dividing the fractional intensities in A by the relative quantum yields of 2, 10 and 26 associated with the corresponding short, intermediate and long lifetimes [7].

tually, in proteoliposomes composed of delipidated (~3 lipids/protein) and non-delipidated (~10 lipids/protein) bacterioopsin and at the high protein/lipid ratio of ~1:40, the probe showed similar λ_{em}^{max}, τ_i, and I_i values (Table 1), indicating no influence of the endogenous lipids on the fluorescence signal. This also confirmed the above conclusion of the absence of any contribution of CHAPS molecules to the probe fluorescence.

The fractional fluorescence intensities associated with the three lifetimes are shown in Fig. 4A and Table 1. They were determined at an emission wavelength of 450 nm where each of the three decays was found to contribute significantly to the total fluorescence. Fig. 4B shows the corresponding probe distribution obtained by dividing the fractional fluorescence intensities associated with the short, medium and long lifetimes by their respective quantum yield Φ_i of 2, 10 and 26 [7]. Bacterioopsin had no influence on the fractional population of probes associated with the intermediate lifetime which remained unchanged at around 20%. In contrast, the fractional population of short-lived species grew markedly from ~47% to ~78% while that of the long-lived ones decreased concomitantly from ~35% to less than 10%. Unlike what was previously found with cholesterol [5], this occurred in a discontinuous way, with two breaks in the plots at protein/lipid ratios of ~1:170 and 1:100 (Fig. 4A,B).

3.3. Fluorescence polarization

To evaluate the influence of the protein on the motional freedom of the lipid acyl chains, the fluorescence anisotropy r of the probe was measured at the temperature of 20°C where the lipids are in the liquid phase. As can be inferred from the data in Table 1, r increased upon addition of bacterioopsin to the lipids. On account of the Perrin equation [32]:

$$r_0/r = 1 + \tau/\varphi$$

Any increase in r may originate either from a decrease in the mean fluorescence lifetime $\langle\tau\rangle$ of the probe (the fluorescence decays are composed of three exponentials) or from an increase in its rotational correlation time φ due to changes in the dynamics of its environment. In this equation, r_0 is the intrinsic anisotropy in the absence of any depolarization process.

As can be observed in Table 1, $\langle\tau\rangle$ decreased upon addition of bacterioopsin to the lipids, which may partly explain the observed increase in r. Let us assume that the protein has no influence on the dynamics of the acyl chains. This leads to the prediction that φ should remain unchanged and therefore (Eq. 3) that $1/r$ should vary linearly with $\langle\tau\rangle$. Actually, and as can be seen in Fig. 5, $1/r$ was observed first to decrease linearly with $\langle\tau\rangle$ upon increasing the protein concentration, up to a protein/lipid ratio of

1:100. Then, an abrupt drop in $1/r$ occurred for the higher protein/lipid ratios of 1:50, 1:40 and 1:25, this large departure from linearity suggesting an increase in φ and therefore a decrease in the dynamics of the lipid acyl chains at these high protein concentrations.

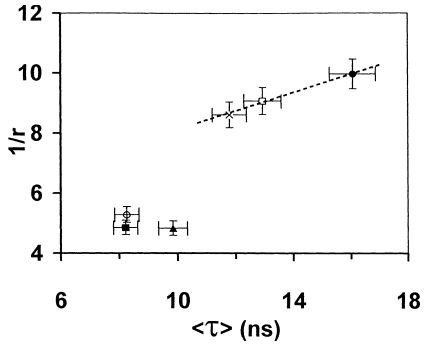

Fig. 5. Plot of $1/r$, the reciprocal of the fluorescence anisotropy measured for anthroyl-PC in egg-PC vesicles in the presence of bacterioopsin at protein/lipid molar ratios of: 0 (●), 1/120 (□), 1/100 (×), 1/50 (▲), 1/40 (○) and 1/25 (■) versus the corresponding mean lifetime $\langle\tau\rangle$.

4. Discussion

As previously observed with cholesterol [5], steady-state fluorescence spectra of anthroyl-PC in egg-PC bilayers indicate changes in the environmental polarity of the probe after addition of bacterioopsin to the lipids. However, these changes may be understood only by analyzing the time-resolved fluorescence data. In the absence of protein, fluorescence decays were well accounted for using three discrete exponentials with corresponding lifetimes of 1.3 ns, 5.8 ns and 20.1 ns, similar to those previously reported for the same lipid [5]. These lifetimes were independent of the fluorescence emission wavelength, thus enabling the corresponding decay associated spectra (DAS) to be obtained and therefore the various local environments of the probe to be clearly specified [5]. The short lifetime of 1.5 ns was associated with a blue ($\lambda_{em}^{max} = 410$ nm) structured DAS, accounting for an environment of low polarity ($\varepsilon \sim 2$), as was expected for the hydrophobic core of the lipid bilayer. The lifetime of 5.5 ns was associated with a green ($\lambda_{em}^{max} = 440$ nm) structureless DAS, indicating a slightly more polar surrounding ($\varepsilon \sim 10$) suggested as corresponding to collisional encountering of probe molecules in the bilayer [5]. A lifetime of 20 ns was the largest measured for the probe in solvents and was detected in the presence of water only [7]. In egg-PC vesicles, it was associated with a red ($\lambda_{em}^{max} = 477$ nm) structureless DAS, accounting for the interaction of the fluorophore with the water molecules trafficking across the lipid bilayer [5]. The weighed sum of these three DAS (on the grounds of the fractional fluorescence intensities) gave the steady-state fluorescence spectrum of origin. In agreement with the well-known influence of cholesterol on the permeability of lipid bilayers to water, addition of this molecule to the lipids resulted in a decrease of the fractional population of fluorophores interacting with water (long-living species) to the benefit of those reporting on an hydrophobic environment (short-living species), and therefore in a blue-shift in the steady-state fluorescence spectra of the probe [5]. Similar although slightly different results were obtained in the presence of bacterioopsin. The three lifetimes remained unchanged around 2 ns, 6 ns and 19–20 ns up to the protein/lipid molar ratio of 1:100 above which the long lifetime progressively decreased to 14–15 ns. Along with a blue-shift in the steady-state fluorescence spectra, the fractional population of the long-living species decreased to the benefit of the short-living ones but in a discontinuous way, with breaks at protein/lipid ratios of 1:170 and 1:100.

As for cholesterol, these results indicate changes in the environmental polarity of the probe within the lipid bilayer [5]. As previously discussed [5], the possibility that this originates from a significant fraction of fluorophore visiting the hydrated polar headgroup region of the bilayer because of thermal fluctuations may be discarded. In anthroyl-PC, the fluorophore is deeply buried in the hydrophobic region of the lipid bilayer, at the level of the C9 carbon atom of the acyl chains [5]. In hydrated DOPC bilayers, the gaussian distribution functions obtained from X-ray and neutron diffraction [33] and molecular dynamics simulation [4,34] experiments for the water and the C9 carbon atom (bearing the double bond) show negligible overlap. From these distribution functions, the mole fraction of fluorophores capable of interacting with the interfacial water may be estimated at less than 0.1%, in marked contrast to the 35% probe molecules

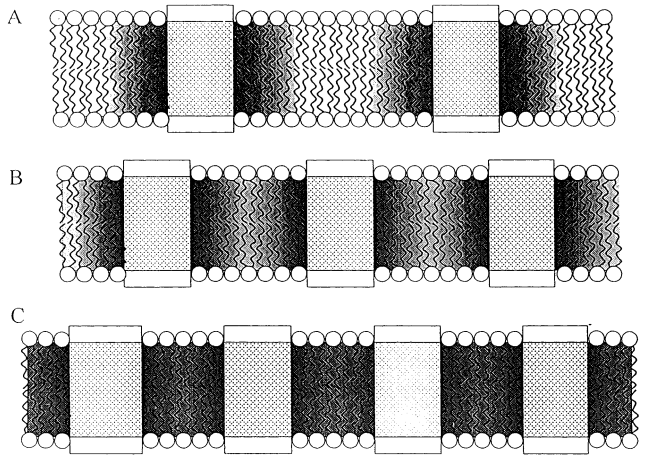

Fig. 6. Schematic drawing of the influence of bacterioopsin on the polarity of the supporting lipid bilayer. The shadowed areas indicate the bilayer regions perturbed by the proteins where lipids exhibit reduced acyl chain dynamics and therefore reduced acyl chain hydration as compared to the bulk lipids. The perturbation is maximum at the contact of the protein and vanishes progressively from the protein surface. In A, which corresponds to protein/lipid ratios $<1:170$, there is no cross-correlation between proteins and the probe anthroyl-PC distributes between perturbed and unperturbed bilayer regions. In B, which corresponds to the protein/lipid ratio of 1:170 (3.5 lipid annuli around each protein on average), cross-correlation starts to be detected and the shadowed regions to overlap. All the lipid molecules are perturbed, but to various extents. In C, which corresponds to the protein/lipid ratio of 1:100 ($\sim$2.5 lipid annuli), near saturation is reached and all the lipid molecules are affected by the protein, nearly to the same extent. For protein/lipid ratios $<1:80$, the protein may be considered in the monomeric state within the lipid bilayer.

found to be associated with water in protein-free egg-PC vesicles.

As previously concluded [5], anthroyl-PC detects the water molecules present in the hydrophobic core of egg-PC bilayers. Our results in the presence of bacterioopsin may be understood using the model in Fig. 6 based on the well-known existence around transmembrane proteins of a shell of lipids with reduced acyl chain motions and consequently with reduced permeability to water as compared to the nonperturbed bilayer regions far from the protein.

With respect to the influence of the protein on the lipid acyl chain dynamics, the perturbation is maximum for lipids in contact with the protein and vanishes exponentially from the protein surface [35–37]. It is characterized by a coherence length ξ in the nanometer range [38] and theoretically it may encompass a rather large number of lipid annuli around the protein (5–6 annuli for $\xi=1.5$ nm [31]). However, and because of the very nature of the exponential decay, the number of lipid annuli effectively seen to be affected by the protein may strongly depend on the sensitivity of the method of detection used. Thus, a large body of NMR and ESR data indicates reduced acyl chain motions mainly at the protein/lipid interface [35–37]. On the other hand, in bacteriorhodopsin/DMPC vesicles, time-resolved fluorescence depolarization and energy-transfer experiments revealed an increase in acyl chain order beyond a distance of 4.5 nm from the protein surface [39]. Using a radius of 1.5 nm for the protein [40] and a molecular area of 0.63 nm^2 for the lipids [41], this corresponds to 5–6 lipid annuli affected by the protein, a result in agreement with the above theoretical predictions. In the present work, an abrupt increase in the fluorescence anisotropy of the probe was detected for bacterioopsin/egg-PC ratios above 1:100. This indicates that on the average, one protein molecule was surrounded by 2–3 annuli of lipids with reduced acyl chain flexibility (according to the above calculation, the first, second and third annulus around the protein are filled with 30, 42 and 55 lipid molecules, respectively).

With respect to the consequences of these perturbations, the permeability of lipid bilayers to water is generally described as a process in which individual water molecules dissolve and then diffuse in the nonpolar region of the bilayer [3]. The diffusion of water [4] and other solutes [42] is often interpreted within the framework of dynamic free-volume theory and as recently shown for nonpolar and spherical solutes by means of molecular dynamics simulation experiments, overall rotation and local isomerization of the acyl chains both contribute to free-volume redistribution within the lipid bilayer [42]. Accordingly, any increase in acyl chain order (or decrease in dynamics) is expected to reduce the bilayer free-volume and dynamics and recent studies do indeed show strong correlation between interchain hydration and acyl chain order [12,43,44]. Free-volume motion (chain isomerization) along the acyl chains is related to the lateral diffusion rate of lipids [3,42] and in the case of water an expression has been derived [3]:

$$P = (V/L^4)D \tag{4}$$

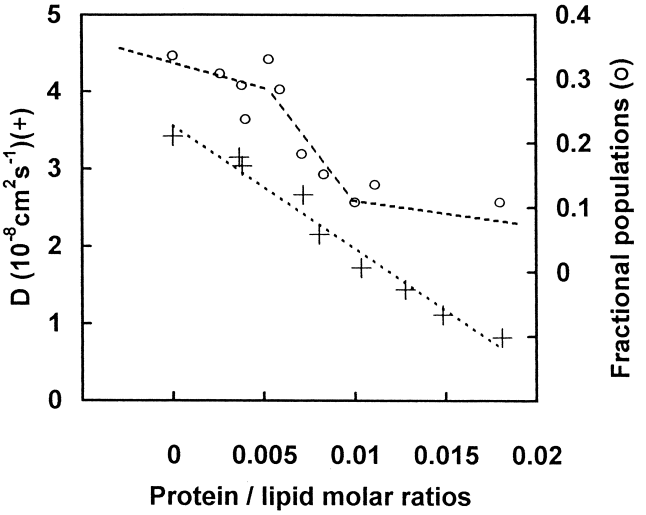

Fig. 7. Comparison of the influence of bacteriorhodopsin on the lateral diffusion coefficient D (+) of lipids in egg-PC multilayers (data taken from [21]) and of bacterioopsin on the fractional population (○) of anthroyl-PC molecules interacting with water in egg-PC bilayers. For the sake of clarity, error bars have been omitted.

which relates the water permeability P of a lipid bilayer to the volume V of a water molecule, the lattice distance L between lipid headgroups and the lateral diffusion coefficient D of lipids. In this respect, membrane proteins are known to affect the lateral motion of lipids. They act as obstacles and also by reducing the self-diffusion coefficients of lipids in their neighborhood [21,45], a result which may be explained within the framework of the free volume theory [45]. In bacteriorhodopsin/egg-PC vesicles, FRAP experiments revealed the presence of a shell of 2–3 lipid annuli around the protein with reduced self-diffusion coefficient [21]. Bacteriorhodopsin and bacterioopsin are structurally closely related and in Fig. 7, it is worth observing that the influence of the former on the diffusion coefficient of lipids follows the influence of the latter on the fractional population of probe molecules interacting with water. From all these observations, one can expect the lipid shell around the protein to be less hydrated than the bulk of the lipids.

With the above in mind, Fig. 6 may be described as follows. At low protein/lipid ratios $<1:170$ (Fig. 6A), bacterioopsin is in the monomeric state [47] and there is no cross-correlation between protein molecules. Anthroyl-PC, which shows no preference for lipids in the ordered or disordered states [5], distributes evenly between the perturbed and unperturbed regions of the lipid bilayer. Marked preference of the probe for the protein may also be discarded from our data. If so, and in contrast to what was observed, the first addition of bacterioopsin to the lipids would have resulted in an abrupt and large increase in the fractional population of probe molecules experiencing a highly hydrophobic and constrained environment, further increase in protein concentration having only little consequence on this fractional population.

Increasing the protein concentration leads to an increase in the fraction of perturbed lipids and therefore in the fractional population of probe molecules experiencing a more hydrophobic environment, and that at the expense of those associated with water. At the protein/lipid ratio of 1:170 which corresponds to $\sim$3.5 lipid annuli around the protein (first break in Fig. 4A,B), cross-correlation between proteins starts to be detected (Fig. 6B). Overlap between perturbed lipid regions is now enough for all the lipid molecules to be significantly affected by the protein. At this stage, any increase in protein concentration leads to a marked increase in protein cross-correlations and therefore in the fraction of strongly perturbed lipids. This explains the marked and concomitant increases and decreases in the fractional populations of probes experiencing an hydrophobic environment and interacting with water, respectively. At the protein/lipid ratio of 1:100 which corresponds to $\sim$2.5 lipid annuli around the protein (second break in Fig. 4A,B), near saturation is reached (Fig. 6C). Bacterioopsin is still in the monomeric form [45] but now cross-correlations between proteins are close to a maximum. Lipid molecules are perturbed nearly to the same extent and all exhibit reduced acyl chain flexibility as assessed by the fluorescence polarization data. The hydrophobic region of the lipid bilayer is poorly hydrated, and any further increase in protein concentration has only minor consequences on the acyl chain flexibility and bilayer hydration. For protein/lipid ratios higher than 1:80, protein aggregation may occur [45]. However, delipidation of bacteriorhodopsin is not favorable to the formation of the trimers which more than likely are at the origin of extensive aggregation of the protein in lipids [46]. In

any case, at the high protein/lipid ratios of 1:40 and above, there is less than one lipid annulus around the protein on the average and all the anthroyl-PC molecules introduced in the lipids are now in contact with the hydrophobic surface of the protein. It is worth stressing that in this case, the fractional population of probe molecules interacting with water is reduced to less than 10%, with a fluorescence lifetime of 14–15 ns only, indicating an environmental polarity much lower than that which prevails in the bulk of the lipid bilayer. Fluorescence studies on gramicidin and apocytochrome *c* reconstituted in lipid vesicles and using DPH as the probe suggested the existence of an hydrated protein/lipid interface for these two proteins [19]. Our data obtained with the help of a specific solvatochromic fluorophore unambiguously located in the hydrophobic core of the lipid bilayer [5] leads to the opposite conclusion. Bacterioopsin strongly affects the hydration of egg-PC bilayers and shows a poorly hydrated protein/lipid interface. These results should be taken into account when discussing the various mechanisms which may contribute to the permeability of biological membranes to water.

References

[1] D. Deamer, J. Bramhall, Chem. Phys. Lipids 40 (1986) 167–188.
[2] S.-J. Marrink, M. Berkowitz, in: E.A. Disalvo, S.A. Simon (Eds.), Permeability and Stability of Lipid Bilayers, CRC Press, Boca Raton, 1995, pp. 21–48.
[3] T. Haines, L.S. Liebovitch, in: E.A. Disalvo, S.A. Simon (Eds.), Permeability and Stability of Lipid Bilayers, CRC Press, Boca Raton, 1995, pp. 123–136.
[4] S.J. Marrink, H.J.C. Berendsen, J. Phys. Chem. 98 (1994) 4155–4168.
[5] E. Pérochon, A. Lopez, J.-F. Tocanne, Biochemistry 31 (1992) 7672–7682.
[6] C.D. Stubbs, C. Ho, S.J. Slater, J. Fluoresc. 5 (1995) 19–28.
[7] E. Pérochon, A. Lopez, J.-F. Tocanne, Chem. Phys. Lipids 59 (1991) 17–28.
[8] E. Pérochon, A. Lopez, J.-F. Tocanne, Chem. Phys. Lipids 58 (1991) 7–17.
[9] A. Carruthers, D.L. Melchior, Biochemistry 22 (1983) 5797–5807.
[10] W.K. Subczynski, A. Wisniewska, J.J. Yin, J.S. Hyde, A. Kusumi, Biochemistry 33 (1994) 7670–7681.
[11] M. Jansen, A. Blume, Biophys. J. 68 (1995) 997–1008.
[12] C. Ho, S.J. Slater, C.D. Stubbs, Biochemistry 34 (1995) 6188–6195.
[13] M.B. Lande, J.M. Donovan, M.L. Zeidel, J. Gen. Physiol. 106 (1995) 67–84.
[14] S. Paula, A.G. Volkov, A.N. van Hoek, T.H. Haines, D.W. Deamer, Biophys. J. 70 (1996) 339–348.
[15] D. Huster, A.J. Jin, K. Arnold, K. Gawrisch, Biophys. J. 73 (1997) 855–864.
[16] J.H. Davis, in: L. Finegold, (Ed.), Cholesterol in Membrane Models, CRC Press, Boca Raton, 1993, pp. 67–135.
[17] A. Milon, T. Lazrak, A.M. Albrecht, G. Wolf, G. Weill, G. Ourisson, Y. Nakatani, Biochim. Biophys. Acta 859 (1986) 1–9.
[18] I.S. Schuler, A. Milon, Y. Nakatani, G. Ourisson, A.M. Albrecht, P. Benveniste, M.A. Hartman, Proc. Natl. Acad. Sci. USA 88 (1991) 6926–6930.
[19] C. Ho, C.D. Stubbs, Biophys. J. 63 (1992) 897–902.
[20] J.F. Tocanne, L. Dupou-Cézanne, A. Lopez, Prog. Lipid Res. 33 (1994) 203–237.
[21] V. Schram, J.-F. Tocanne, A. Lopez, Eur. Biophys. J. 23 (1994) 337–348.
[22] M. Bloom, I.C.P. Smith, in: A. Watts, J.J. De Pont (Eds.), Progress in Protein–Lipid Interactions, vol. 1, Elsevier, Amsterdam, 1985, pp. 61–88.
[23] D. Marsh, in: A. Watts, J.J. De Pont (Eds.), Progress in Protein–Lipid Interactions, vol. 1, Elsevier, Amsterdam, 1985, pp. 143–172.
[24] D. Oesterhelt, W. Stoeckenius, Methods Enzymol. 31 (1974) 667–678.
[25] F. Dumas, M.M. Sperotto, M.C. Lebrun, J.-F. Tocanne, O.G. Mouritsen, Biophys. J. 73 (1997) 1940–1953.
[26] G.L. Peterson, Anal. Biochem. 83 (1977) 346–356.
[27] B.R. Eaton, E.A. Denis, Arch. Biochem. Biophys. 176 (1976) 604–609.
[28] R.A. Klein, Biochim. Biophys. Acta 210 (1970) 486–491.
[29] S. Mazères, V. Schram, J.-F. Tocanne, A. Lopez, Biophys. J. 71 (1996) 327–335.
[30] J.B.A. Ross, C.J. Schmidt, L. Brand, Biochemistry 20 (1981) 4369–4377.
[31] B. Piknova, E. Pérochon, J.-F. Tocanne, Eur. J. Biochem. 218 (1993) 385–396.
[32] J.R. Lakowicz, in: Principles of Fluorescence Spectroscopy, Plenum Press, New York, 1983, pp. 132–134.
[33] M.C. Wiener, S.H. White, Biophys. J. 61 (1992) 434–447.
[34] S.E. Feller, D. Yin, R.W. Pastor, A.D. MacKerell Jr., Biophys. J. 73 (1997) 2269–2279.
[35] B.R. Lentz In: R.C. Aloia, C.C. Curtain, L.M. Gordon (Eds.), Advances in Membrane Fluidity, Lipid Domains and Relationship to Membrane Function, vol. 2, A.R. Liss, New York, 1988, pp. 141–161.
[36] M. Bloom, E. Evans, O.G. Mouritsen, Q. Rev. Biophys. 24 (1991) 293–397.
[37] D. Marsh, L.I. Horvath, Biochim. Biophys. Acta 1376 (1998) 267–296.
[38] F. Jâhnig, Biophys. J. 36 (1981) 329–345.

[39] M. Rehorek, N.A. Dencher, M.P. Heyn, Biochemistry 24 (1985) 5980–5988.
[40] N. Grigorieff, T.A. Cesta, K.H. Downing, J.M. Baldwin, R. Henderson, J. Mol. Biol. 259 (1996) 393–421.
[41] J.F. Nagle, Biophys. J. 64 (1993) 1476–1481.
[42] T.X. Xiang, J. Phys. Chem. B 103 (1999) 385–394.
[43] H. Huster, A.J. Jin, K. Arnold, K. Gawrisch, Biophys. J. 73 (1997) 855–864.
[44] P.F.F. Almeida, W.L.C. Vaz, T.E. Thompson, Biochemistry 31 (1992) 7198–7210.
[45] N.A. Dencher, K.D. Kohl, M.P. Heyn, Biochemistry 22 (1983) 1323–1334.
[46] B. Sternberg, P. Gale, A. Watts, Biochim. Biophys. Acta 980 (1989) 117–126.
[47] T. Gulik-Krzywickz, M. Seigneuret, J.L. Rigaud, J. Biol. Chem. 262 (1987) 15580–15588.